High-resolution inversion for Helicopter-borne TEM data for lead-zinc mineralised body detection

X. Wu[1,2,3], G. Xue[1,2,3], Y. Pang[4], Z. Ni[2,4], G. Fang[4], Y. He[1,2,3] and K. Lei[1,2,3]

[1] *The Key Laboratory of Mineral Resources, Institute of Geology and Geophysics, Chinese Academy of Sciences, Beijing, China*

[2] *University of Chinese Academy of Sciences, Beijing, China*

[3] *The Institutions of Earth Science, Chinese Academy of Sciences, Beijing, China*

[4] *The Institute of Electronics, Chinese Academy of Sciences, Beijing, China*

ABSTRACT   At present, one-dimensional regularisation inversion is the main way to extract underground electrical structure information in mainstream Helicopter-borne Transient Electromagnetic (HTEM) detections. The reliability requirements for the initial model of the regularisation inversion method is relatively low, and the inversion could be appropriate for different types of targets by choosing different stable functionals, for example, the minimum gradient support functional is generally considered to be suitable for objects with sharp boundaries. However, when there are several low-resistivity layers within a limited depth region, the existing methods have still difficulty in distinguishing each layer. For this reason, this paper draws on the layer stripping inversion concept in seismic data inversion, and proposes a piecewise locking inversion method based on the existing regularisation inversion. This method combines the advantages of the regularisation inversion and the Marquardt inversion, and avoids the interference of late data to shallow target recognition by data segmentation. Lastly, through the application for the simulated and measured data in a lead-zinc mining area, this paper proves that this method can effectively improve the resolution of the HTEM one-dimensional inversion to the adjacent low-resistivity layers.

Key words: HTEM, inversion, piecewise locking, regularisation.

1. Introduction

Helicopter-borne Transient Electromagnetic Method (HTEM) is a kind of transient electromagnetic detection method that, by using helicopters, can effectively overcome the limitation of topographical and geomorphic conditions (such as mountains, deserts, water network dense areas, forest vegetation coverage areas, etc.), where the traditional detections on the ground are difficult to carry out quickly. Therefore, HTEM has the characteristics of high efficiency and economy, and is widely used in resource exploration such as metal ore, groundwater, and geothermal, as well as environmental engineering, marine topographic survey, and polar research (Fountain and Smith, 2003; Macnae and Nabighian, 2005; Allard, 2007).

At present, widely used HTEM systems include: VTEM (Witherly *et al.*, 2004), SkyTEM (Sørensen and Auken, 2004) and HeliTEM (Mulè *et al.*, 2012).

Compared with the traditional ground methods, as a flight observation method, HTEM introduces disturbance factors such as motion noise and flight attitude effects and so on, which are generally not encountered in ground methods. On the other hand, the aeronautical adaptive design of the HTEM system under the constraints of the flight platform performance parameters, such as the power supply and the carrying capacity, will also affect the quality of the observed signals. Therefore, the entire data processing process of HTEM will be much more difficult than the traditional ground methods, and roughly includes (but not limited to): line data interception, (near source) sferics processing (Leggatt *et al.*, 2000), motion-induced noise removal (Macnae *et al.*, 2008; Wang *et al.*, 2015), system response removal (Legault *et al.*, 2012; Schamper *et al.*, 2014), stacking and windowing (Auken *et al.*, 2007; Nyboe and Sørensen, 2012). Through these steps, the various types of noise entering the observation data will be suppressed, the attitude effect caused by the system in flight observation will be corrected, and the performance defects introduced by the hardware system due to the aerodynamic adaptive design will be "remedied" to some extent.

After data processing, the distribution information of the underground medium is extracted through imaging or inversion methods. Different from inversion, the imaging does not include the optimisation process required for inversion, but performs some transformation on the observation data (Wolfgram and Karlik, 1995; Macnae *et al.*, 1998; Yin *et al.*, 2015), such as apparent resistivity, apparent depth, etc., to realise the rapid extraction of geoelectric information, so it is very suitable for the quick assessment of the target-occurrence situation in the field. In contrast, the purpose of the inversion is to solve the geoelectric model by fitting the transient electromagnetic decay curve sparsed by the windowed data, and provide a basis for subsequent geological interpretation (Zhdanov, 2009). According to the dimensional assumptions of the source and the heterogeneity and anisotropy of the Earth's medium, the inversion method can be easily divided into one-dimensional inversion and multi-dimensional inversion. Multi-dimensional inversion can provide more detailed information on the distribution of underground media (Raiche *et al.*, 2001; Wilson *et al.*, 2006). However, due to a large amount of data for HTEM detection, the multi-dimensional inversion normally takes a long time, and, meanwhile, the accuracy is difficult to control, so the multi-dimensional inversion is still in development. (Cox and Zhdanov, 2008; Cox *et al.*, 2012; Oldenburg *et al.*, 2013; Yang *et al.*, 2014). Considering that multi-dimensional inversion is not yet fully developed, the currently widely used HTEM services mainly adopt one-dimensional inversion, and quasi two-dimensional and quasi three-dimensional inversion based on one-dimensional inversion (Auken and Christiansen, 2004; Viezzoli *et al.*, 2008; Siemon *et al.*, 2009; Monteiro Santos *et al.*, 2011). In terms of specific optimisation methods, since the inverse problem of TEM is an ill-posed problem, its inversion usually adopts the regularisation inversion method (Tikhonov, 1999; Zhdanov, 2009). In the regularisation inversion, three functionals are usually involved: parametric functional, misfit functional, and stabilising functional, in which the parametric functional is composed of misfit functional and stabilising functional. The function of the stabilising functional is to limit the solution process based on the misfit functional to a specific model space so as to ensure the rationality of the solution. This rationality derives from the understanding of the real Earth's structure, such as: for some structures with sedimentary

features, the variation of the Earth's resistivity has a certain gradual variation; or for some structures with rock mass intrusion characteristics, the resistivity sometimes changes abruptly. On this basis, the researchers proposed some stabilising functionals with different properties, including: maximum smoothness stabilising functional (Constable *et al*., 1987; Smith and Booker, 1991), modified total variation stabilising functional (Acar and Vogel, 1994; Vogel and Oman, 1998), and minimum gradient support functional (Portniaguine and Zhdanov, 1999).

As for metal detection, because the ore body and the boundary of surrounding rock (that is resistivity discontinuity) is generally obvious, the Marquardt inversion (Levenberg, 1944; Marquardt, 1963) is traditionally used to extract the information of target position and resistivity with relatively high precision and fast convergence speed. The premise of using Marquardt inversion to obtain high-quality inversion results is a high-quality initial model, but it is difficult to obtain a high-quality initial model in unknown regions, which limits the application of Marquardt inversion. Compared with the Marquardt inversion, the focus regularisation inversion method based on Minimum Gradient Support (MGS) functional can distinguish the discontinuous boundary of resistivity better without depending on the initial model, so this method becomes the main choice of HTEM inversion.

In 2017, CAS-HTEM system developed by the Chinese Academy of Sciences carried out a test flight in a mining area in north-eastern Inner Mongolia, China. The basic rock in this area is diorite, and mineralised bodies occur in the contact zone between the basic rocks and other rocks. Through the study of inversion results, it is found that under specific underground structure conditions, the focus inversion method based on MGS functional cannot effectively distinguish adjacent low resistivity layers (the detailed situation will be described in the next section). Analysing the problem and referring to the concepts of layer stripping inversion technology in seismic data (Yagle and Levy, 1985; Wang *et al*., 2011; Vassiliou *et al*., 2015), we propose a new piecewise locking inversion method based on the decay curve. This method combines the advantages of the regularisation inversion and the Marquardt inversion, and avoids the interference of late data to shallow target recognition by data segmentation. Lastly, through the application for the simulated and measured data, this paper proves that this method can effectively improve the resolution of the HTEM one-dimensional inversion to the adjacent low-resistivity layers.

2. Method

2.1. Regularisation inversion

Firstly, the regularisation inversion method is briefly reviewed. Generally, the inversion problem can be described as solving the following equations:

$$d = A(m), \tag{1}$$

where d is the observation data, m is the description of the Earth resistivity distribution, and A is the forward operator. In the inversion of transient electromagnetic data, the above problem is often ill-posed, then according to the regularisation theory, the parametric functionals can be written as follows:

$$P^\alpha = \phi(m) + \alpha s\,(m), \tag{2}$$

where α is regularisation parameter, $\phi(m)$ is the misfit functional, it is defined as follows:

$$\phi(m) = \|Am - d\|^2, \tag{3}$$

where $s(\mathrm{m})$ represents stabilising functional, several common types of stabilising functional are defined as:

$$s_1\left(m\right) = \left\|\nabla m\right\|^2 = \left(\nabla m, \nabla m\right) = \min, \tag{4}$$

$$s_2\left(m\right) = \int_V \sqrt{\left|\nabla m\right|^2 + \beta^2}\, dv, \tag{5}$$

$$s_3\left(m\right) = \int_V \frac{\nabla m \cdot \nabla m}{\nabla m \cdot \nabla m + \beta^2}\, dv = \mathrm{spt}\nabla m - \beta^2 \int_V \frac{1}{\nabla m \cdot \nabla m + \beta^2}\, dv, \tag{6}$$

where s_1, s_2, s_3 represent maximum smoothness stabilising functional, modified total variation stabilising functional, and minimum gradient support functional, respectively, and β represents a small value, $\mathrm{spt}\nabla m$ represents the combined closed subdomains of the model parameter space V.

Based on the above definition, the regularisation inversion parametric functional can be defined by the following formula:

$$P^\alpha\left(m, d\right) = \left\|W_d A\left(m\right) - W_d d\right\|^2 + \alpha\left\|W_m m - W_m m_{apr}\right\|^2, \tag{7}$$

where W_d and W_m represent a certain weighted matrix of data and model respectively. Obviously, the definition of W_m is related to the selected stability functional, and M_{apr} represents the initial model.

The solution of the minimisation value in parametric functional is achieved by solving the first variation of parametric functional equal to zero. When forward operator A is a non-linear operator, the inversion problem is non-linear. For the least squares inversion of non-linear regularisation problems, common methods include: steepest descent method, Newton method, and conjugate gradient method. Newton's method can be used as an example to briefly introduce the general process. The model modification quantity Δm is introduced firstly, and the relationship between the adjacent iteration steps is as follows:

$$m_{n+1} = m_n + \Delta m. \tag{8}$$

The parametric function is rewritten and solving the first variation:

$$
\begin{aligned}
\delta_{\Delta m} P^\alpha\left(m_{n+1}, d\right) &= \delta_{\Delta m} P^\alpha\left(m_n + \Delta m, d\right) \\
&= \left(\delta \Delta m\right)^T \left[F_{m_n}^T W_d^T W_d\left(Am_n + F_{m_n}\Delta m - d\right) + \alpha W_m^T W_m\left(m_n + \Delta m - m_{apr}\right)\right]
\end{aligned}
\tag{9}
$$

where F_{m_n} is the Fréchet derivative matrix of forward operator A at m_n step. So, the parametric functional gain the minimum value, when the inner part in the right of Eq. 9 is equal to zero. Therefore, the solution of the inverse problem described in Eq. 1 can be obtained by solving the

solution of Eq. 9 when the inner part of the right bracket equals zero and by several iterations until the result reaches the convergence condition.

In addition, for the linear inversion problem, and when $W_d=W_m=I$, the inversion problem changes into the classical Levenberg-Marquardt damped least squares inversion method.

2.2. Problem analysis

Although the Marquardt inversion has a high precision for the simple layered model, the reliability of the results depends too much on the initial model. The regularisation inversion is, therefore, regarded as the main method in the inversion of CAS-HTEM data.
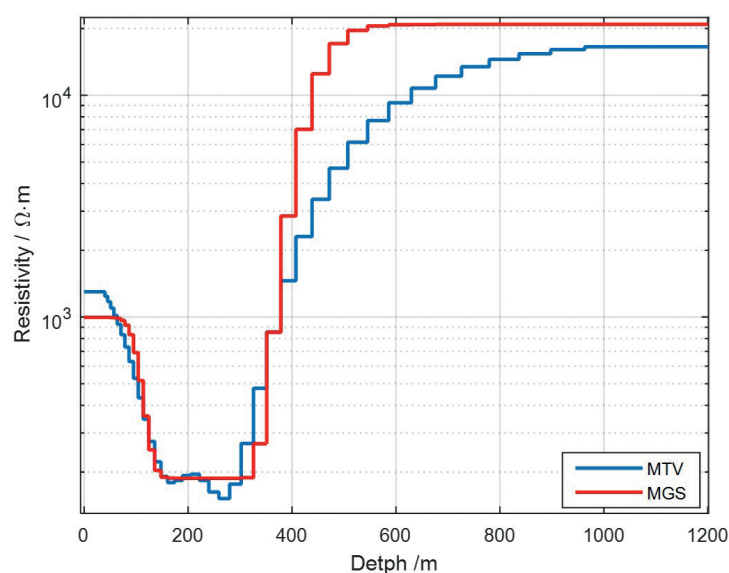
Fig. 1 - Inversion results comparison between MTV and MGS stabilising functional.

In 2016, CAS-HTEM system was developed by Institute of Electronics, Chinese Academy of Sciences. In 2017, a test flight was conducted in a mining area in north-eastern Inner Mongolia, China. The basic rock in this area is diorite, and mineralised bodies occur in the contact zone between the basic rocks and other rocks. A comparison between the inversion results by using MGS and MTV (Modified Total Variation) stabilising functional respectively of a measurement point in this experiment is shown in Fig. 1. MTV functional is also a stabilising functional suitable for block structure. It can be seen from the figure that the whole geoelectric structure can be considered as an H-shaped structure with one low resistivity layer sandwiched between two high resistivity layers. By comparing the inversion results of using MGS and MTV stabilising functional, it is concluded that the MGS stabilising functional has better control over a wide range of high and low resistivity regions, and the boundary of the low resistivity region is clearer than that of MTV stabilising functional. Further study on the low resistivity region of the inversion results shows that the one using MTV stabilising functional has a K-type secondary structure with one high resistivity layer sandwiched between two low resistivity layers in the low resistivity region of the main H-shaped structure, while the result using MGS stabilising functional cannot distinguish the corresponding secondary structure. By analysing

the K-type secondary structure in the result using the MTV stabilising functional, it is concluded that: 1) the resistivity contrast between low and high resistivity layers may not be great; 2) the resistivity of the three layers in the secondary structure is relatively low compared with the high resistivity part of the main H-shaped structure. This shows that the resistivity of the secondary structure in the low resistivity area changes slightly compared with the significant resistivity contrast of the external bedrock. The MGS stabilising functional has effectively extracted the significant resistivity contrast in the main structure, but it has not effectively extracted the secondary structure in the low resistivity region. The possible reason is that: because of the introduction of the MGS functional, its function makes the main H-structure strengthened, and the low-resistivity part contained therein is considered to be a block structure as a whole, which weakens the resolution of the internal fine structure within the low resistivity part by the inversion method.

Table 1 - Parameters of the Earth model.

Layer	Resistivity (Ωm)	thickness (m)
1	1400	150
2	180	20
3	500	120
4	100	20
5	10000	

In order to solve the above problem, the simplest idea is that the bottom high resistivity layer of the H-type main structure is expected to have no influence on the shallow inversion. In order to verify this idea, we designed an Earth structure model with five layers (Table 1), which includes an H-type main model and a K-type secondary structure in the low resistivity part of the H-type structure. The main parameters of the response model include: unit transmitter current, single-turn transmitter loop (radius is 15 m), unit effective observation area of the search coil and 50-m flight altitude. The time window is defined as 40 logarithmic equidistant time points from 10 μs to 10 ms. The calculation layers are 40 layers, the top layer thickness is 50 m, the layer thickness progressive base is 5 m, and the layer thickness progressive increment coefficient is 1.07. The focus inversion method based on MGS stabilising functional is adopted to the whole decay curve and its first 10 windows respectively, and the results are shown in Fig. 2. It can be seen from the figure that the fine structure in the middle cannot be effectively identified by the inversion of the whole decay curve, while the identification of the shallow low resistivity layer can be realised by using data of the early windows, although there are some resistivity oscillations above the low resistivity layer. Based on this, and taking the Marquardt inversion into consideration to further enhance the resolution of inversion, we propose the piecewise locking inversion method.

2.3. Piecewise locking method

Considering the simplest case, the whole decay curve will be divided into two parts (as shown in Fig. 3): assuming that a pretreated decay curve contains N sampling windows, and the L-th window is selected as the piecewise point.
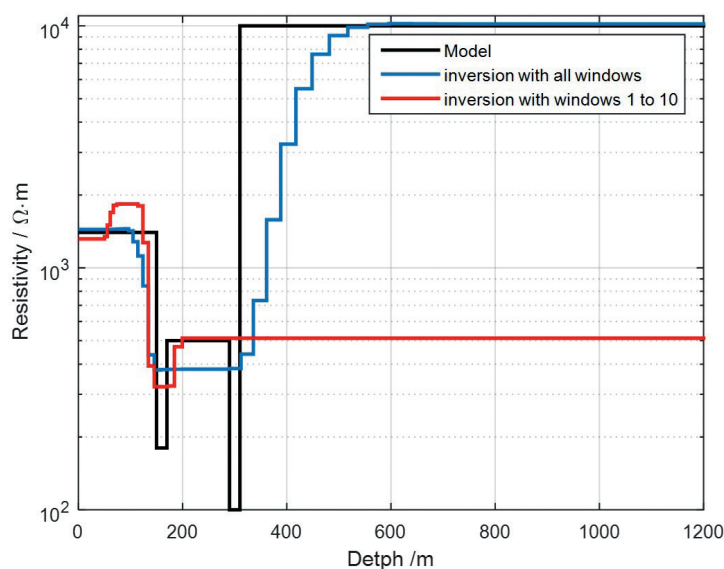
Fig. 2 - Inversion results with all windows of the decay curve and only the windows 1 to 10.

The basic procedure of the piecewise locking inversion method is: firstly, the shallow model is obtained by regularisation inversion using data d_{1L} which contains the data from window 1 to L; then, the data d_{1N} from window 1 to N (i.e. all data) is used for inversion, but in the inversion process, the shallow model obtained from the inversion of d_{1L} data is solidified and locked in the inversion, that is, the shallow model is only used to synthesise the decay curve, but its value is not modified. In practice, we can choose multiple segmentation points to obtain multiple sets of data according to the situation.
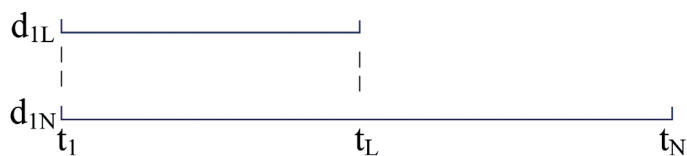
Fig. 3 - Data segmentation of a single decay curve.

The key to realising the piecewise locking inversion is to lock the shallow inversion results. Continue the above assumptions of dividing into two parts and assume that the inversion depth space is H = [h_1, h_2, …, h_q], that is, the inversion object is an Earth model with q layer with resistivity m = [ρ_1, ρ_2, …, ρ_q]. Using the d_{1L} data, the inversion results of the whole q-layer can be obtained because the inversion depth space is H, but it is easy to find that only the shallow x layer is reliable from the inversion results (which will be demonstrated in the next section by an example). That is to say, in the inversion process of data d_{1N}, the shallow x layer resistivity, i.e. [ρ_1, [ρ_2, …, [ρ_x] will be solidified and locked in the following way:

1) in theory, the regularisation inversion does not depend on the initial model, so for the regularisation inversion, a uniform half-space whose resistivity is ρ_{hs} is usually used as the initial model. For the hypothetical q-layer Earth, the initial model is m_0 = [ρ_{hs}, ρ_{hs}, …, ρ_{hs}]. Before inversion with the data d_{1N}, the initial model will be modified according to

the inversion results using the d_{1L} data, and the resistivity of shallow *x* layer equals to the shallow model obtained from inversion of the d_{1L} data $[\rho_{L1}, \rho_{L2}, \ldots, \rho_{Lx}]$, which forms the initial model $m_0 = [\rho_{L1}, \rho_{L2}, \ldots, \rho_{Lx}, \rho_{hs}, \ldots, \rho_{hs}]$;

2) locking the shallow *x*-layer resistivity model, that is, do not involve the shallow *x*-layer in the correction calculation, only adopt it to synthesise the whole decay curve. Therefore, it is necessary to restrict the various vectors and matrices involved in the calculation.

In the *n*-th iteration, assuming that the model parameters from layer *x*+1 to layer *q* are $m_{n(x+1:q)}$, rewrite the stabilising functional after adjusting the roughness matrix correspondingly. Take the MGS stabilising functional as an example:

$$W_m = \frac{1}{\sqrt{\nabla m_{n(x+1:q)} \cdot \nabla m_{n(x+1:q)} + \beta^2}}, \tag{10}$$

Fréchet derivative matrix F_{m_n} should be an $N \times q$ matrix, where N is the number of windows contained in d_{1N} data and q is the original number of layers. The process of locking the shallow *x*-layer resistivity model involves two steps: the first step is to calculate Fréchet derivative matrix, the second step is to delete the *x* column related to the shallow *x*-layer, and get Fréchet derivative matrix $F_{m_{n(x+1:q)}}$ for bottom layer *x*+1 to layer *q*, which is a $N \times (q-x)$ matrix.

By rewriting the stabilising functional and the Fréchet derivative matrix, we can calculate the $m_{n+1(x+1:q)}$ only using the model parameters $m_{n(x+1:q)}$ from bottom layer *x*+1 to layer *q*. After obtaining $m_{n+1(t+1:q)}$, combine it with the shallow locked *x* layer resistivity model to get m_{n+1}:

$$m_{n+1} = [m_{n+1(1:x)} \ m_{n+1(x+1:q)}]. \tag{11}$$

In practice, in order to further improve the resolution of inversion results, after completing the regularisation inversion using d_{1L} data, we will simplify the shallow *x*-layer model into a simple layered model (generally, no more than 5 layers). Then, regard it as the initial model, and perform the Marquardt inversion to the d_{1L} data. In fact, we provide a more reliable initial model for Marquardt inversion using the regularisation inversion result, and obtain a more accurate inversion result using the Marquardt inversion.

By the Marquardt inversion of d_{1L} data, the thickness and resistivity of the simple layered model will be modified, and finally we can obtain a simple layered model M_{SL} (including depth and resistivity) corresponding to the depth of the original *x*-layer model. The original *q*-layer model is adjusted by using the thickness information of each layer included in the model M_{SL} instead of the original shallow *x*-layer. In this way, in the subsequent inversion of d_{1N} data, the depth model will be rewritten as follows:

$$H_s = [H_{SL} \quad H_{t+1} \quad L \quad H_q], \tag{12}$$

where H_{SL} contains the depth information of the shallow limited layers contained in the model M_{SL}. Accordingly, the iteration of parameter modification is also changed into:

$$m_{n+1} = [m_{n+1(SL)} \ m_{n+1(t+1:q)}], \tag{13}$$

where $m_{n+1(SL)}$ contains the resistivity information of shallow limited layers contained in the model M_{SL}.

Based on the above introduction, the process of the piecewise locking inversion method can be summarised as follows: 1) performing inversion using the whole decay curve to estimate the position of the piecewise points; 2) segmenting the windowed data of decay curve; 3) performing regularisation inversion for the early segmentation; 4) simplifying the inversion result of the early segmentation and extracting a simple layered model; 5) using this simple layered model as the initial model to perform the Marquardt inversion for the early segmentation; 6) locking the results of the early segmentation Marquardt inversion into the initial model of subsequent segmentation; 7) performing regularisation inversion of the late segments; 8) simplifying the regularisation inversion results of late segmentation, and extracting a simple layered model that includes the shallow simple layered model which has been solidified; 9) taking the simple layered model as the initial model, and performing Marquardt inversion again for late segmentation to obtain the final results; 10) if the number of segmentation more than two, repeating the above steps until the Marquardt inversion result of the whole decay curve is obtained.

Two aspects should be added: 1) in the segmentation point selection, besides observing the inversion result of the whole decay curve and estimating the locations of the segmentation points, an adaptive algorithm based on the piecewise time constant estimation can also be used to segment the whole attenuation curve; 2) the stabilising functional used in the piecewise locking inversion is not limited to MGS. According to the prior knowledge of geological structure, other stabilising functionals such as maximum smoothing functional or MTV functional can also be selected.

3. Numerical example

3.1. Synthetic example

In this example, the geoelectric model and the forward and inverse calculation parameters are consistent with Fig. 1. According to the inversion results of Fig. 2, the whole decay curve can be divided into two segmentations in window 10. According to the regularisation inversion results of the first 10 windows in Fig. 2, a simple layered model is extracted by a simple envelope method shown in Fig. 4.
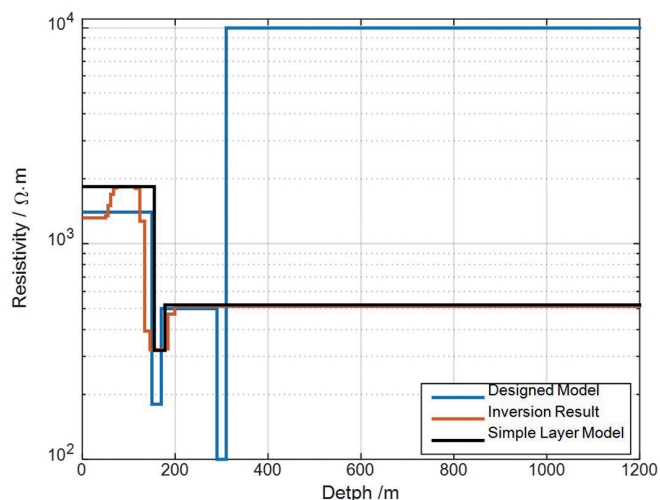
Fig. 4 - Extract of the simple layer model from the result of the regularisation inversion.

Take the simple layered model shown in Fig. 4 as the initial model, perform the Marquardt inversion to the data of the first 10 windows, and the result is shown in Fig. 5. It shows that although the method used to extract the initial model from the regularisation inversion result is rough, the location and resistivity of the top high resistivity layer and the first low resistivity layer have been clearly distinguished after the Marquardt inversion.
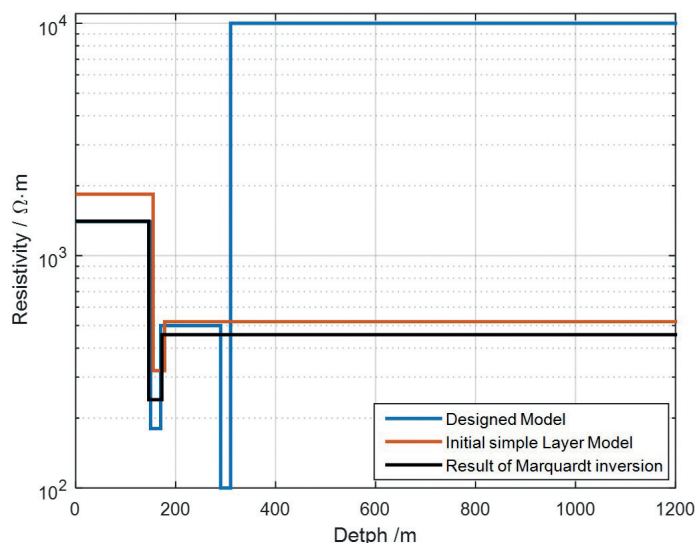
Fig. 5 - Result of the Marquardt inversion of the first data segment.

So far, we have obtained the resistivity of the top three layers and the thickness of the top two layers by the Marquardt inversion, while the thickness of the third layer and the information of the layers below the third layer are still unknown. Regarding the resistivity of the top three layers and the thickness of the top two layers as known information and locking them in accordance with the method introduced in this paper. Then perform the focus inversion based on MGS stabilising functional to the whole decay curve, and the result is shown in Fig. 6. We can find
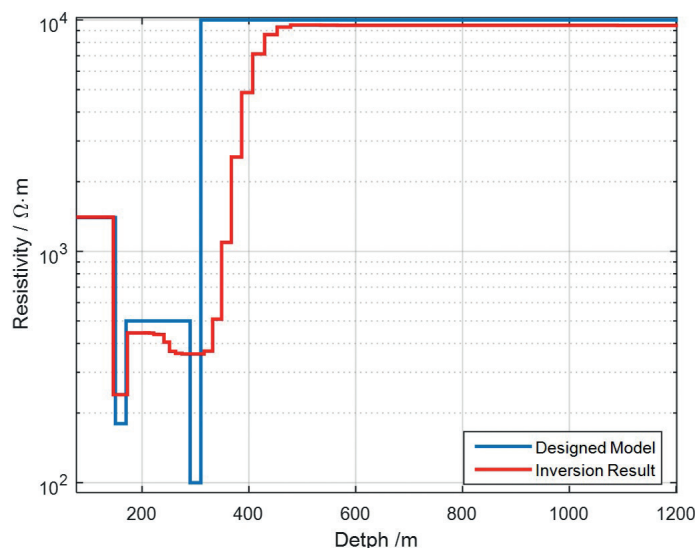
Fig. 6 - Result of regularisation inversion with the piecewise locking method.
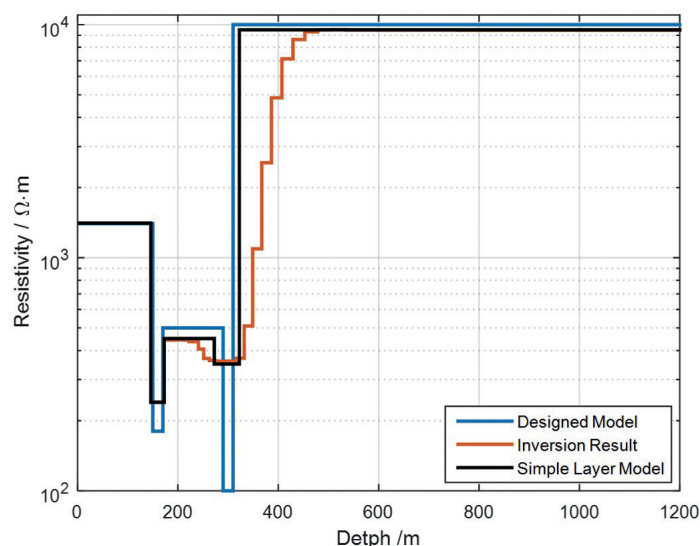
Fig. 7 - Extract of the simple layer model from the result of the regularisation inversion of the whole decay curve.

that there is another low resistivity layer below the shallow low resistivity layer. Simple layered models of the deep layers are also extracted by a simple envelope method, and the result is shown in Fig. 7.

Take the simple layered model extracted from the above process as the initial model to the Marquardt inversion, and the result is shown in Fig. 8. In Fig. 8, we compare the inversion result of the piecewise locking method with the result of the traditional method. It can be seen that the traditional inversion cannot clearly identify the geoelectric information of two adjacent low resistivity layers, while adopting the piecewise locking inversion can reflect the fine geoelectric structure of adjacent low resistivity layers. In addition, the resolution to the depth and resistivity of shallow low resistivity layers is higher by piecewise locking inversion, but for deep low resistivity layers, they are still not very precise. Further research shows that this may be related to the resolution that the late data can achieve, and may be further improved
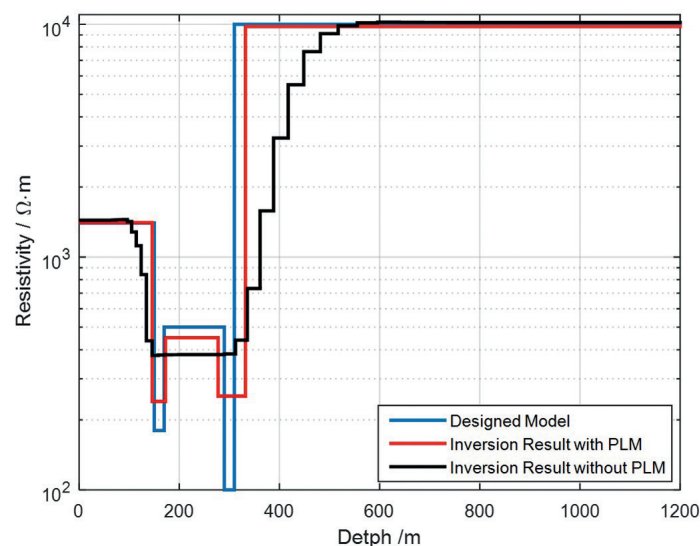
Fig. 8 - Comparison of inversion result with and without the piecewise locking method.

by choosing a more appropriate regularisation functional and optimising the algorithm for obtaining simple layered models from the regularisation inversion result. In addition, the windowing density of the decay curve can also be increased under the condition of SNR (signal to noise ratio), which helps to achieve a more detailed piecewise locking inversion.

3.2. Field data example

The CAS-HTEM is a central loop system. The main parameters are as follows: the peak transmitting current is 250 A, the radius of the transmitting loop is 14 m, four turns, the noise level is 0.1 nT/s, and the sampling rate of the receivers is 128 kHz.

After completing the development and integration test of CAS-HTEM system, we conducted a test flight in a mining area in north-eastern Inner Mongolia (as shown in Fig. 9). The test region, with an area of 11.87 km^2, is located in the eastern Wuzhumuqin Banner of Xilinhot City, Inner Mongolia Autonomous Region, about 180 km away from Uriyastai, where the
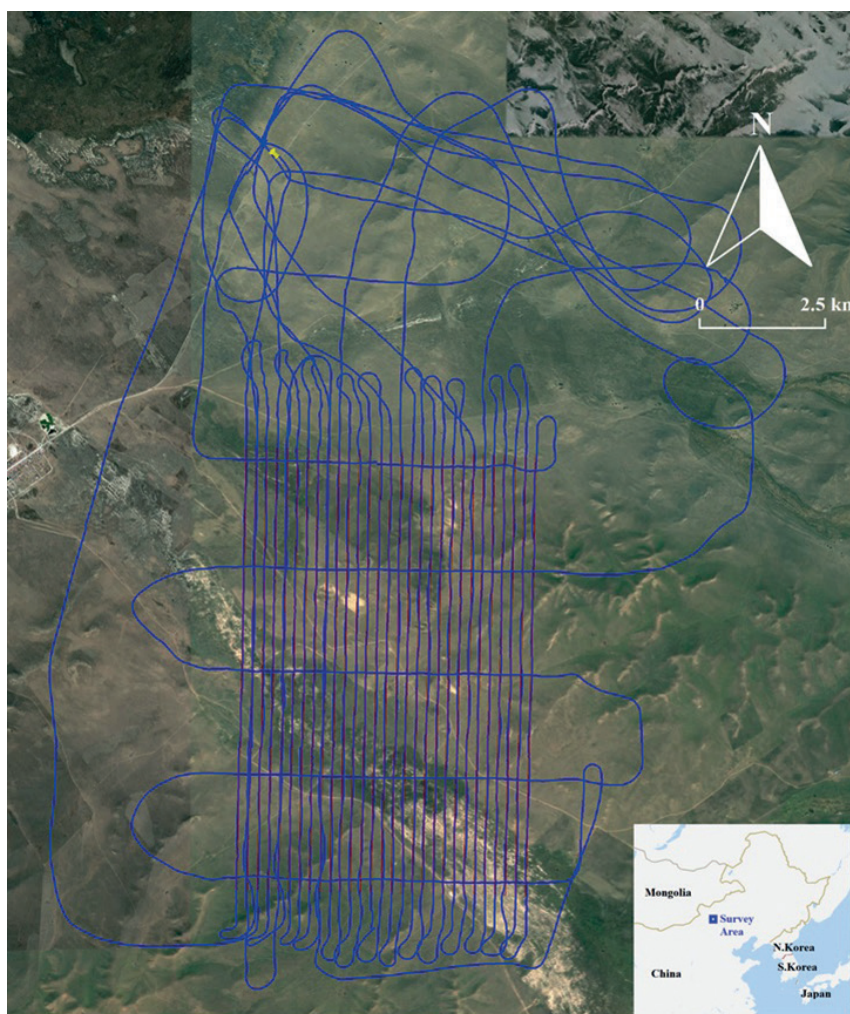
Fig. 9 - The survey area and flight lines.

banner government is located. Lead-zinc mineralisation was discovered in the previous drilling. Take one typical drilling as an example, the hole is 450 m deep and passes through many mineralised layers, and the roof of the top mineralised layer is about 226 m away from the surface. Mineralised bodies occur in granite porphyry and clastic rocks such as quartz sandstone or siltstone in contact with them, average grade: Zn 1.943%, Pb 1.45%.

The survey area was about 50 km². It was designed totaling 29 N-S lines (8.5 km line length, 200 m line spacing) and 5 E-W lines (5.6 km line length, 2 km line spacing). The temporary landing zone of the helicopter (location of the pin) was located about 5 km north of the survey area.

The measuring point No. 178 of line 13 is selected for inversion. The main parameters are as follows: flight height is 51.2 m, transmitter base frequency is 25 Hz, actual peak transmitter current peak is 185 A, the system noise level is 0.1 nT/s, the sampling rate is 128 kHz. Perform the focus regularisation inversion based on the MGS stabilising functional and the piecewise locking inversion of the data, respectively, the results are shown in Fig. 10. In addition, there is an early drill hole near the measuring point with a depth of 450 m, and its lithology information is shown in the histogram on the right side of the inversion results.

Drill Hole	No.	Depth (m)	Thickness (m)	Lithology
	1	9.80	9.80	Quaternary
	2	102.95	93.15	Diorite
	3	190.35	87.40	Granite Porphyry
	4	226.40	36.05	Diorite
	5	229.30	2.90	Mineralized body
	6	232.30	3.00	Diorite
	7	233.30	1.00	Mineralized body
	8	237.30	4.00	Diorite
	9	271.40	34.10	Mineralized body
	10	287.40	16.00	Diorite
	11	297.90	10.50	Mineralized body
	12	450.00	152.10	Granodiorite
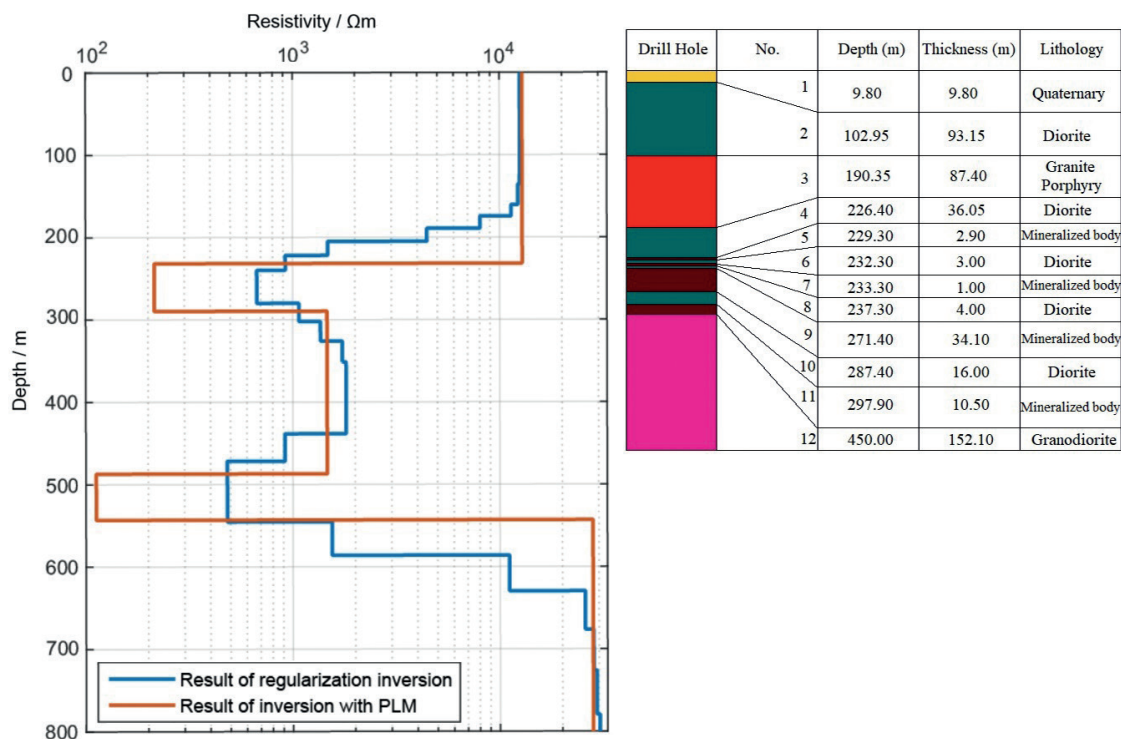
Fig. 10 - Inversion results and lithologic histogram.

As shown in Fig. 10, because the distance between the two low resistivity layers is relatively large, the focus algorithm based on MGS stabilising functional can also roughly find the low resistivity structures underground, while the piecewise locking method can distinguish the low resistivity structure underground more clearly. From the lithologic histogram, it can be seen

that mineralisation exists between 226.4 and 297.9 m, and in the piecewise locking inversion result, the shallow low resistivity layer is observed between 214.5 and 289.7 m, which is in good agreement with drilling data. Besides, Fig. 10 shows that there is another low resistivity layer at a depth of about 500 m, and the mineral owner had been advised to verify it in the follow-up work.

4. Conclusion

Based on the traditional regularised inversion method, a piecewise locking inversion method is proposed in this paper, which combines the advantages of regularisation inversion and the Marquardt inversion, and uses the data segmentation method to avoid the interference of late data (deep information) on shallow target recognition, thus effectively improving the resolution of inversion to adjacent low resistivity layers. When performing the piecewise locking inversion, the decay curve should be segmented reasonably, and the early segmentation should be inverted individually. The obtained shallow geoelectric model is solidified and, then, brought into subsequent segmentation inversion. When the data of Earth segmentation is inverted, a regularisation inversion is used to obtain the initial model for the Marquardt inversion. The final result of entire decay curve is obtained by means of segment-by-segment advancement. Through the application for the simulated and measured data, this paper proves that this method can effectively improve the resolution of the HTEM one-dimensional inversion to the adjacent low resistivity layers. In future work, it is proposed to gradually promote this method to multi-dimensional inversion.

REFERENCES

Acar R. and Vogel C.R.; 1994: *Analysis of total variation penalty methods*. Inverse Problems, **10,** 1217-1229.

Allard M.; 2007: *On the origin of the HTEM Species*. In: Proc. Exploration 07, 5th Decennial International Conference on Mineral Exploration, Toronto, Canada, pp. 355-374.

Auken E. and Christiansen A.V.; 2004: *Layered and laterally constrained 2D inversion of resistivity data*. Geophys., **69**, 752-761.

Auken E., Westergaard J., Christiansen A.V. and Sørensen K.I.; 2007: *Processing and inversion of SkyTEM data for high resolution hydrogeophysical surveys*. In: Extended Abstracts 19th International Geophysical Conference and Exhibition, Australian Society of Exploration Geophysicists, Perth, Australia**,** 4 pp., doi: 10.1071/ASEG2007ab007.

Constable S.C., Parker R.C. and Constable G.G.; 1987: *Occam's inversion: a practical algorithm for generating smooth models from EM sounding data*. Geophys., **52**, 289-300.

Cox L.H. and Zhdanov M.S.; 2008: *Advanced computational methods for rapid and rigorous 3D inversion of airborne electromagnetic data*. Commun. Comput. Phys., **3**, 160-179.

Cox L.H., Wilson G.A. and Zhdanov M.S.; 2012: *3D inversion of airborne electromagnetic data*. Geophys., **77**, WB59-WB69.

Fountain D. and Smith R.; 2003: *55 years of AEM; 50 years of KEG!*. Paper presented at the meeting of KEGS 50th Anniversary Symposium, Toronto, Canada.

Legault J., Prikhodko A., Dodds D., Macnae J. and Oldenborger G.A.; 2012: *Results of recent VTEM helicopter system development testing over the spiritwood valley aquifer, Manitoba*. In: Proc. 25th Symposium on the Application of Geophysics to Engineering and Environmental Problems, Tucson, AR, USA, pp. 114-130, doi: 10.4133/1.4721712.

Leggatt P.B., Klinkert P.S. and Hage T.B.; 2000: *The spectrum airborne electromagnetic system - further developments*. Geophys., **65**, 1976-1982.

Levenberg K.; 1944: *A method for the solution of certain nonlinear problems in least squares*. Q. Appl. Math., **2**, 164-169.

Macnae J. and Nabighian M.; 2005: *Electrical and EM methods, 1980-2005*. The Leading Edge, **24**, 42-45.

Macnae J., King A., Stolz N., Osmakoff A. and Blaha A.; 1998: *Fast AEM data processing and inversion*. Explor. Geophys., **29**, 163-169, doi: 10.1071/EG998163.

Macnae J., Ley-Cooper Y. and Davis A.; 2008: *HEM calibration and bird-swing correction: an insular example*. In: Stark T.J. (ed), SEG Technical Program Expanded Abstracts 2008, pp. 1318-1322, doi: 10.1190/1.3059158.

Marquardt D.W.; 1963: *An algorithm for least squares estimation of nonlinear parameters*. J. Soc. Ind. Appl. Math., **11**, 431-441.

Monteiro Santos F.A., Triantafilis J. and Bruzgulis K.; 2011: *A spatially constrained 1D inversion algorithm for quasi-3D conductivity imaging: application to DUALEM-421 data collected in a riverine plain*. Geophys., **76**, B43-B53.

Mulè S., Carter S. and Wolfgram P.; 2012: *Advances in helicopter airborne electromagnetics*. In: Extended Abstracts 22nd International Geophysical Conference and Exhibition, Australian Society of Exploration Geophysicists, Brisbane, Australia, vol. 12, 3 pp., doi: 10.1071/ASEG2012ab306.

Nyboe N.S. and Sørensen K.I.; 2012: *Noise reduction in TEM: presenting a bandwidth- and sensitivity-optimized parallel recording setup and methods for adaptive synchronous detection*. Geophys., **77**, 203-212.

Oldenburg D.W., Haber E. and Shekhtman R.; 2013: *Three dimensional inversion of multisource time domain electromagnetic data*. Geophys., **78**, E47-E57.

Portniaguine O. and Zhdanov M.S.; 1999: *Focusing geophysical inversion images*. Geophys., **64**, 874-887.

Raiche A., Annetts D. and Sugeng F.; 2001: *EM target response in complex hosts*. In: Extended Abstracts 15th International Geophysical Conference and Exhibition, Australian Society of Exploration Geophysicists, Brisbane, Australia, 4 pp.

Schamper C., Auken E. and Sørensen K.I.; 2014: *Coil response inversion for very early time modelling of helicopter-borne time-domain electromagnetic data and mapping of near-surface geological layers*. Geophys. Prospect., **62**, 658-674.

Siemon B., Auken E. and Christiansen A.V.; 2009: *Laterally constrained inversion of helicopter-borne frequency-domain electromagnetic data*. J. Appl. Geophys., **67**, 259-268.

Smith J.T. and Booker J.R.; 1991: *Rapid inversion of two- and three dimensional magnetotelluric data*. J. Geophys. Res., **96**, 3905-3922.

Sørensen K.I. and Auken E.; 2004: *SkyTEM? A new high-resolution helicopter transient electromagnetic system*. Explor. Geophys., **35**, 194-202.

Tikhonov A.N.; 1999: *Mathematical geophysics*. Moscow State University, Moscow, Russia, 476 pp.

Vassiliou A., Sandberg K., Beylkin G., Lewis R.D., Popovic I. and Woog L.; 2015: *Layer stripping migration velocity analysis using accurate survey sinking*. In: Extended Abstracts 85th Annual International Meeting, Society of Exploration Geophysics, New Orleans, LA, USA, pp. 4222-4226, doi: 10.1190/segam2015-5917235.1.

Viezzoli A., Christiansen A.V., Auken E. and Sørensen K.I.; 2008: *Quasi-3D modeling of airborne TEM data by spatially constrained inversion*. Geophys., **73**, F105-F113.

Vogel C.R. and Oman M.E.; 1998: *Fast, robust total variation-based reconstruction of noisy, blurred images*. IEEE Trans. Image Process., **7**, 813-824.

Wang B., Ji J., Yoon K., Cai J., Whiteside W., Mason C. and Li Z.; 2011: *Layer-stripping RTM based on wavefield redatuming*. In: Extended Abstracts 81st Annual International Meeting, Society of Exploration Geophysics, San Antonio, TX, USA, pp. 3280-3284.

Wang Y., Smith R., Zhu K., Lin J. and Chen B.; 2015: *HTEM noise frequency characteristics simulation and influencing analysis*. In: Proc. International Workshop on Gravity, Electrical & Magnetic Methods and Their Applications, Chengdu, China, pp. 398-401, doi: 10.1190/GEM2015-103.

Wilson G.A., Raiche A.P. and Sugeng F.; 2006: *2.5D inversion of airborne electromagnetic data*. Explor. Geophys., **37**, 363-371.

Witherly K., Irvine R. and Morrison E.; 2004: *The Geotech VTEM time-domain helicopter EM system*. In: Extended Abstracts 74th Annual International Meeting, Society of Exploration Geophysics, Denver, CO, USA, vol. 25, pp. 1217-1220.

Wolfgram P. and Karlik G.; 1995: *Conductivity-depth transform of GEOTEM data*. Explor. Geophys., **26**, 179-185.

Yagle A.E. and Levy B.C.; 1985: *A layer-stripping solution of the inverse problem for a one-dimensional elastic medium*. Geophys., **50**, 425-433.

Yang D.K., Oldenburg D.W. and Haber E.; 2014: *3-D inversion of airborne electromagnetic data parallelized and accelerated by local mesh and adaptive soundings*. Geophys. J. Int., **196**, 1492-1507.

Yin C.C., Zhang B., Liu Y.H., Ren X.Y., Qi Y.F., Pei Y.F., Qiu C.K., Huang X., Huang W., Mia J.J. and Cai J.; 2015: *Review on airborne EM technology and developments*. Chin. J. Geophys., **58**, 2637-2653.

Zhdanov M.S.; 2009: *Geophysical electromagnetic theory and methods*. Elsevier, Amsterdam, The Netherlands, vol. 43, 868 pp.

Corresponding author: Guoqiang Xue
The Key Laboratory of Mineral Resources, Institute of Geology and Geophysics,
Chinese Academy of Sciences
19 Beitucheng Western Road, Chaoyang District, Beijing 100029, China
Phone: +86 10 82998193; e-mail: ppxueguoqiang@163.com